

Hole Structure and Its Formation in Thin Films of Hydrolyzed Poly(styrene maleic anhydride) Alternating Copolymers

MINGTAI WANG, XIAOGUANG ZHU, LIDE ZHANG

Institute of Solid State Physics, Chinese Academy of Sciences, Hefei 230031, People's Republic of China

Received 5 January 1999; accepted 20 May 1999

ABSTRACT: Maleic anhydride moieties on the backbone chains of poly(styrene maleic anhydride) alternating copolymer (SMA) hydrolyzed in a THF solution containing water and hydrochloric acid. Well-arrayed holes were obtained in spin-cast thin hydrolyzed SMA films on a single crystal silicon wafer, and the hole diameter and its distribution were measured with AFM data. Results showed that the hole size was almost uniform, and was influenced by water content when spin speed was kept unchanged. The THF solution with a SMA concentration of about 1 g/mL and weight ratio H₂O/SMA of 1/3 produced holes having an average diameter of 0.60 μm and depth of 206.12 nm, when cast at a spin speed of 1400 rpm. It was noted that the formation of the holes in thin hydrolyzed SMA film was different from the dewetting process in thin homopolymer films, but was associated with the intrinsic properties of the copolymer forming the films. The surfactant effect of hydrolyzed SMA was suggested to interpret the formation of the holes. The holes were described to be the traces of water droplets that were emulsified by the hydrolyzed SMA during casting. © 2000 John Wiley & Sons, Inc. *J Appl Polym Sci* 75: 267–274, 2000

Key words: styrene–maleic anhydride copolymer; atomic force microscopy; thin polymer film; surface pattern

INTRODUCTION

Generally speaking, films of thickness less than 1000 angstroms (\AA) are classified as ultrathin films, and of thickness between 1000 and 10000 \AA are regarded to as thin films.¹ More recently, many studies on surface pattern of spin-cast thin and ultrathin films are carried out in polymer/polymer blends by using a three-composition or ternary system: two polymers in a common solvent.^{2–6} When the thin blend films are annealed at a temperature

above T_c (critical temperature of polymer blend), a hole or bicontinuous spinodal decomposition surface pattern can be formed. The formation of these surface patterns is often regarded as a tracking-phase separation process within these films under the induction of temperature. Ermi et al.³ showed that droplets having a higher surface tension than the surrounding medium are expected to cause evaluations in the polymer–air boundary, while droplets of a lower surface tension should lead to depressions in the film surface, resulting in a hole structure. However, the holes in these thin blend films are often irregularly arrayed and not uniform in diameter.^{2,3,7}

Hole structures in the thin films were also observed in polystyrene homopolymer films on silica

Correspondence to: M. Wang.
Contract grant sponsor: The National Nature Science Foundation of China.

Journal of Applied Polymer Science, Vol. 75, 267–274 (2000)
© 2000 John Wiley & Sons, Inc. CCC 0021-8995/00/020267-08

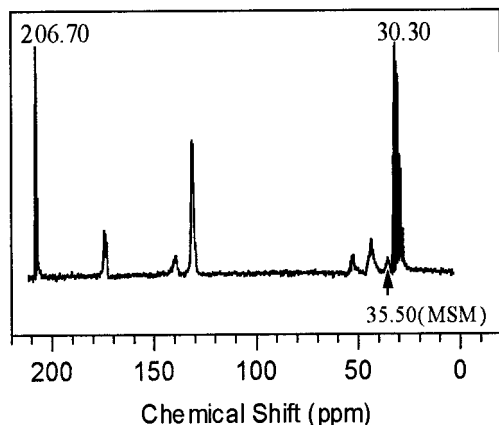


Figure 1 ^{13}C -NMR spectrum for the styrene-maleic anhydride alternating copolymer (SMA).

substrates by Reiter,⁸ when the films were annealed at a temperature above the glass transition temperature, T_g , of polystyrene. The formation of these holes was interpreted in terms of dewetting substrate. Thin and smooth polystyrene films become unstable when annealed at a temperature above its T_g . Modulations of the surface induced by thermal fluctuations may increase in amplitude and eventually hit the substrate. Hence, such films are expected to break up and to minimize the area where the liquid has contact with the substrate by a dewetting process.

In studies, we found that thin hydrolyzed SMA films spin-cast on inorganic substrates, such as silicon wafer, quartz, and glass slide, can exhibit well-arrayed and almost uniform holes without temperature induction. The holes in the thin films are expected to be potential for submicrometer or nanometer fabrications. These films may act as templates for the formation of well-arrayed submicro/nanocrystal domains, as in the cases of ceramic templates, for example, an alumina template,^{9,10} or of a polymethylmethacrylate hole template made with electron beam lithography.¹¹ In present article, the hole structure in hydrolyzed SMA thin films on single crystal silicon wafers is described, and a formation process of the holes is suggested.

EXPERIMENTAL

Synthesis and Chain Structure of SMA

Styrene and maleic anhydride usually produce equimolar copolymers for a major part of the

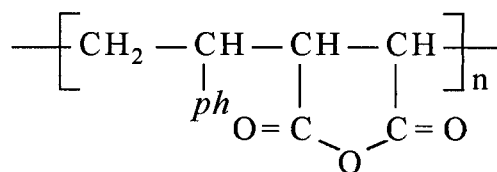
monomer feed composition range. Only at high styrene concentrations in the feed are styrene sequences of a length greater than one produced.¹²⁻¹⁴ SMA used in this study was synthesized in benzene using a 1 : 1 molar monomer feed and benzoyl peroxide (recrystallized before use) as initiator, as described elsewhere.¹⁵

The mol fraction, χ , of styrene in the copolymer is 0.51, determined from an integrated ^1H -NMR spectrum of SMA, as described elsewhere.¹⁶ Figure 1 is a ^{13}C -NMR spectrum of the copolymer. The assignments of carbon resonances in ^{13}C -NMR spectra for the copolymers of styrene and maleic anhydride have been well made by other authors^{14,17}; the resonance signal at 35.50 ppm is regarded as the characteristic resonance of MSM (M: maleic anhydride; S: styrene) triad sequence on the backbone chain.¹⁴ NMR results revealed that the copolymer as-synthesized is an alternating one, and the structure of SMA can be shown by Scheme 1.

Preparation of Thin Films on Si Substrate

SMA was dissolved in THF (purified and distilled over sodium) overnight at room temperature to form the SMA solutions with SMA concentrations of 1-2% g/mL. The pH value of the SMA solution was adjusted to the range of 1-1.5 with concentrated hydrochloric acid (37%), then deionized water of a suitable weight was charged in and stirred for 2 h to hydrolyze SMA at room temperature, and obtain the sample solution (labeled as HSMA). On the other hand, only an appropriate quantity of deionized water was added into the SMA solution and stirred for 2 h at room temperature to obtain the sample without addition of HCl (labeled as SMA-H₂O).

Thin films were spin coated onto precleaned single-crystal silicon wafers with a root mean square (RMS) roughness of 2.90 Å at a spin speed of 1400 rpm (8 s). This procedure resulted in films with a mean thickness of about 230-235 nm when the SMA concentration was 1% g/mL, eval-



Scheme 1

uated from ellipsometric measurements. Prior to spin coating, the single crystal silicon wafers were treated at 80°C for 1.5 h with "piranha solution," a 30 : 70 mixture of 30% hydrogen peroxide and concentrated sulfuric acid, followed by extensive rinsing with deionized water, and a final rinsing with absolute ethanol, and drying.

Instruments and Measurements

The number-average molecular weight (M_n) of the as-synthesized copolymer (SMA) was 2560, and the $M_w/M_n = 1.04$, determined with a Waters 150-C gel permeation chromatography (GPC) with acetone as the solvent and monodispersed polystyrene as the standard sample. The ^{13}C -NMR spectrum of the copolymer was recorded on a FX-90Q NMR spectrometer (22.5 MHz ^{13}C) at 50°C with acetone- d_6 as the solvent and internal standard (signals at 30.30 and 206.70 ppm) using a $\phi = 10$ -mm NMR tube, and the concentration of the acetone- d_6 solution was approximately 10% g/mL.

FTIR spectra were recorded on a Nicolet Magna-IR™ 750 spectrometer with a maximum resolution of 0.1 cm^{-1} . Samples for FTIR were in the form of films obtained from THF solutions and dried at 80°C under vacuum for 2 days before test.

The glass transition temperature (T_g) of SMA was 217°C. The T_g was measured on a Perkin-Elmer DSC-2C apparatus as follows, with the DSC calibrated with ultrapure indium: the SMA sample (7–8 mg) was heated at 570 K for 3 min to eliminate the thermal history, and quenched to 240 K, then scanned from 240 to 550 K with a heating rate of 20 K/min. The T_g was taken as the midpoint of the heat capacity change.

Thin films were placed in a desiccator with silica-gel drier until atomic force microscopy (AFM) measurements (ca. for 2–3 days). An AutoProbe® CP Proven Performance, Research SPM (Park Scientific Instruments) was used to acquire the topographical AFM images in a noncontact mode using silicon cantilevers with a conical tip, which has a typical radius of 100 Å supplied by the manufacturer. The tip cantilevers in the dimension of $85 \times 28 \times 1.8 \mu\text{m}^3$ have a force constant of 18 N cm^{-1} and resonant frequency of 360 kHz. AFM observations were executed in the air condition.

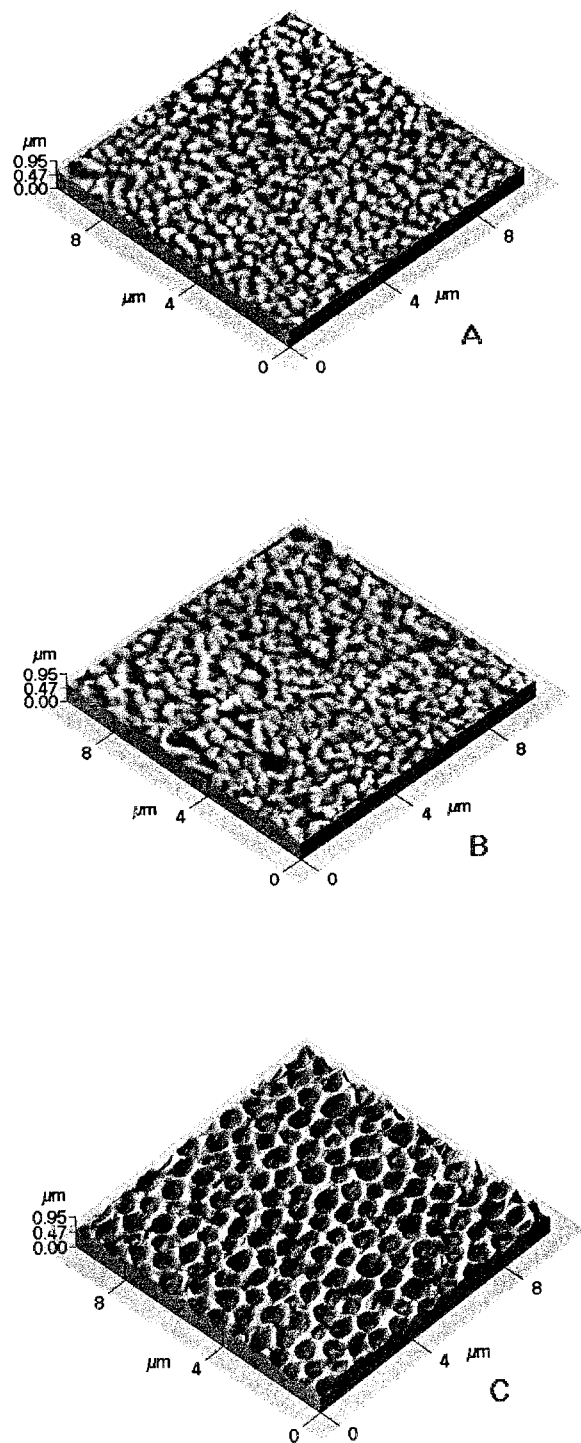


Figure 2 AFM images of thin films cast from different THF solutions with a SMA concentration of 1% g/mL, and the weight ratio of $\text{H}_2\text{O}/\text{SMA}$ for sample SMA- H_2O and HSMA was 1/3. (A) SMA in dried THF, RMS roughness = 232 Å; (B) SMA- H_2O , RMS roughness = 246 Å; (C) HSMA.

RESULTS AND DISCUSSION

Observation of the Hole Structure

Figure 2 shows typical AFM images of spin-cast thin SMA, SMA-H₂O, and HSMA films. It is known that a bicontinuous pattern similar to spinodal decomposition is the characteristics of thin SMA and SMA-H₂O films [Fig. 2(A) and (B)],^{3,4} but the bicontinuous pattern changes into well-arranged “holes” in the HSMA film [Fig. 2(C)], and these holes are almost uniform in diameter. Surface patterns in Figure 2(A) and (B) are mainly attributed to the difference in the surface free energy ν between end groups and units on the backbone chains of SMA.¹⁶ The discussions of this article focus on the hole structure.

Figure 3 shows the 2D image of Figure 2(C) and the cross-sectional view along the line in the AFM image. The hole structure was also observed by SEM (SEM not provided here). Low-magnification views of the specimen surface by SEM re-

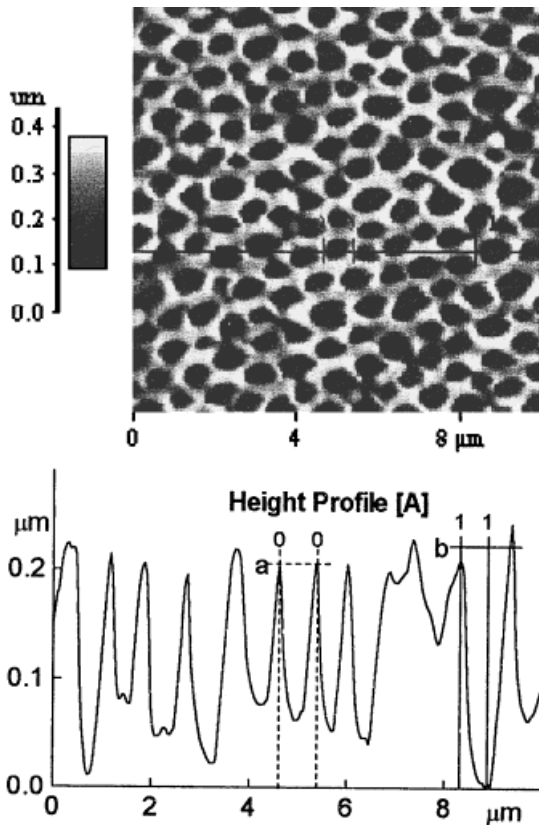


Figure 3 Two-dimensional AFM image (above) and sectional view along the line in the image (below) for the sample HSMA in Figure 2.

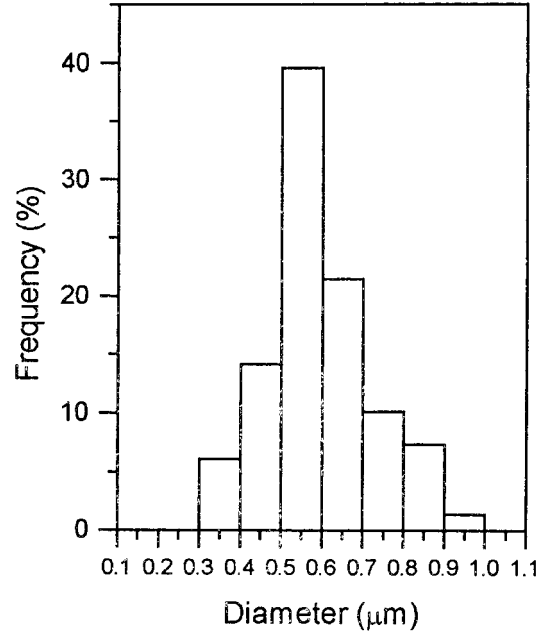


Figure 4 Histogram showing the distribution of the hole diameters in the image area of $10 \times 10 \mu\text{m}^2$ for sample HSMA in Figure 2, and data were obtained from Figure 3.

vealed the hole pattern is in a large area. The 2D AFM image was analyzed to obtain the diameter and its distribution of holes in the image area, i.e., $10 \times 10 \mu\text{m}^2$. Here, the diameter of a hole is defined as the distance between two vertical boundary lines in the cross-sectional view, for example, 0–0, as shown by Figure 3; while the depth as the height from the bottom to the upper part of the hole, as shown by the right vertical line 1 and the horizontal line b in Figure 3.

With the data obtained from Figure 3, the hole diameter and its distribution histogram were obtained and plotted in the Figure 4. The height of an interval in the histogram is the ratio of the number of holes with diameters within the range in the interval over the total hole number. The average diameter \bar{d} for holes in the whole image area is estimated by the equation

$$\bar{d} = \frac{1}{N} \sum_{i=1}^{n_0} d_i n_i \quad (1)$$

where d_i is the diameter of holes in the i th interval of the histogram, n_i the number of the holes with a diameter of d_i in the i th interval, n_0 the total number of intervals, and

$$N = \sum_{i=1}^{n_0} n_i \quad (2)$$

The standard deviation S_d of the hole diameter is determined by the formula

$$S_d = \left\{ \frac{1}{N-1} \sum_{i=1}^N (d_i - \bar{d})^2 \right\}^{1/2} \quad (3)$$

From eqs. 1–3, the holes in the image area have an average diameter of 0.60 μm , with S_d of 0.13 μm . From Figure 4 it can be known that about 62% of the holes are in a diameter range of 0.50–0.70 μm .

The mean hole depth of the holes was evaluated by replacing the diameter by the depth value in eqs. 1–3. Measurements were carried out by using 50 holes on the cross-sectional views at different horizontal positions, and the average AFM hole depth \bar{h} is 206.12 nm, with a standard deviation S_h of 6.73 nm. It is noted that the depth may be a real value, because the diameters of the holes were much larger than that of the conical tip, and the geometry of conical tip (the sectional triangle of it has a 4 μm height and 20° tip angle) could enable the tip enter the holes.

Formation of the Hole Structure

Thermal induction is an important external factor for the formation of holes in the dewetting process of the styrene homopolymer.⁸ The as-shown surface patterns in Figure 2 were formed during casting, and can be observed once casted. It is obvious that holes in the thin HSMA film were not a result of temperature induction, because the film was not specially treated after casting at any temperature above room temperature, for example, at 217°C, the T_g of SMA. The formation of the holes in the hydrolyzed SMA thin films should follow a different mechanism from dewetting, and the surface pattern changes in Figure 2 should be associated with the intrinsic properties of the copolymer forming the films, namely, with the chemical reactions in sample preparations.

Hydrolysis of SMA in the Acidified THF Solution

The samples in Figure 2 were measured by an FTIR spectrometer to determine the chemical reactions that may take place during preparation,

and the respective IR spectrum for them is shown in Figure 5.

The adsorption bands at 1858 and 1778 cm^{-1} in Figure 5(A) are characteristic bands of SMA,¹⁸ assigned to asymmetrical and symmetrical $\nu_{\text{C}=\text{O}}$ of maleic anhydride moieties, respectively. Bands at 1600, 1500, and 1450 cm^{-1} are the $\nu_{\text{C}=\text{C}}$ of the phenyl groups on the backbone chains. The band at 1214 cm^{-1} is attributed to the $\nu_{\text{C}-\text{O}-\text{C}}$ of maleic anhydride units, referring to the $\nu_{\text{C}-\text{O}-\text{C}}$ band at 1310–1210 cm^{-1} for a five-numbered cyclo-anhydride.¹⁹ The band at 700 cm^{-1} is the $\delta_{\text{C}=\text{C}}$ of the phenyl groups, which can be used as an internal reference to offset differences in the thickness of the IR samples.

Figure 5(C) reflects the IR information on the hydrolysis of SMA. The appearance of an adsorption band at 1710 cm^{-1} is due to the $\nu_{\text{C}=\text{O}}$ of the carboxylic acid groups derived from maleic anhydride moieties.^{18a} The strong bands at 1440–1395 and 1320–1210 cm^{-1} is attributed to the $\nu_{\text{C}-\text{O}}$ and $\delta_{\text{O}-\text{H}}$ adsorption of the derived carboxylic acid groups, respectively, referring to the small molecular carboxylic acid.¹⁹ At the same time, a broad absorbance around 3000 cm^{-1} also indicates the existence of —COOH groups in the hydrolyzed SMA.

It is known²⁰ that carboxylic acid dimers due to strong hydrogen bonding in saturated aliphatic acids display very broad and intense O—H

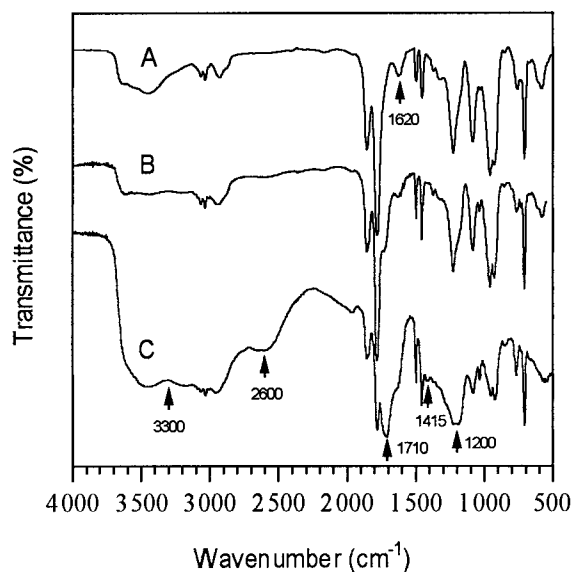
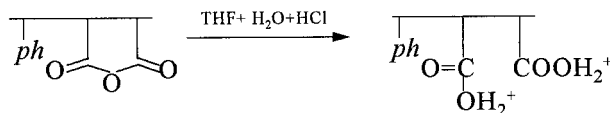


Figure 5 FTIR spectra for samples in Figure 2. (A) SMA; (B) SMA-H₂O; (C) HSMA.



Scheme 2

stretching absorption in the region of 3300–2500 cm^{-1} , which differs from the strong absorption of a free hydroxyl stretching vibration (near 3560–3500 cm^{-1}); and the band usually centers near 3000 cm^{-1} . Particularly, these carboxylic acid dimers always show the O–H stretching vibration at 2600 cm^{-1} caused by the strong hydrogen bonding.^{19,20a} So the IR sample (i.e., hydrolyzed SMA in solid state) exhibits a strong hydrogen bonding effect between —COOH groups, which is indicated by the absorption band at 2600 cm^{-1} and the more broad absorbance around 3000 cm^{-1} , and also by the red shift of the $\nu_{\text{C=O}}$ of carboxylic acid groups from near 1760 (without a hydrogen bond) to around 1710 cm^{-1} (with a hydrogen bond).^{20a}

In the region of 3700–2310 cm^{-1} of Figure 5(C), a very broad peak is observed. Obviously, this absorption region is much wider than that for usual $\nu_{\text{O-H}}$ in carboxylic acid dimers (i.e., 3300–2500 cm^{-1}). Factors causing this broad peak are complex. We think the widening comes from the influence of carbon dioxide and water absorbed in measurement, because carbon dioxide^{20a} has absorption bands at 3700–3500 cm^{-1} and 2380–2220 cm^{-1} , and water¹⁹ has absorption around 3500 cm^{-1} . The existence of absorbed water in the IR samples can also be indicated¹⁹ by the band at 1620 cm^{-1} .

The bands of carboxylic acid groups (e.g., 1710 cm^{-1}) are weak for the SMA–H₂O sample [Fig. 5(B)]. It is evident that SMA in the SMA–H₂O system hydrolyzed only to a small degree within the time (i.e., 2 h) for hydrolysis of SMA, and hydrochloric acid can accelerate the hydrolysis of SMA. The SMA hydrolyzes in the acidified THF solution containing water, and can be shown by Scheme 2.

As viewed from organic chemistry, the protonation of —COOH groups, perhaps not all of them on the backbone chains, is believed here, even though no direct evidences are provided. The protonation will impart influence on the conformation of HSMA chains in solution (refer to the discussion below).

Formation of the Hole Structure

The formation of holes can be explained by the surfactant effect of hydrolyzed SMA. As a polymer surfactant, the polymer should not dissolve in water, and have groups that are hydrophilic and can enter the water phase. The hydrolyzed SMA in the present article dissolves slightly in water, and hardly in acidified water,¹⁵ and its carboxylic acid groups are hydrophilic. In addition, the M_n of SMA (i.e., 2560) is not large; this shows that the hydrolyzed SMA will be of a low molecular weight. Thus, it is not doubted that our hydrolyzed SMA has properties of an anionic polymer surfactant.^{21,22}

In the solution state, hydrogen bonding between —COOH groups should be taken into consideration. Our experiments have shown that the holes in hydrolyzed SMA films result from the existence of both carboxylic acid groups on the backbone chains and HCl in the solution; the HCl especially is crucial for the formation of holes.¹⁶ This phenomenon should be attributed to the effect of hydrogen bonding between —COOH groups in the solution state. Details of the hydrogen bonding effect will appear in another article.

It can be understood that such hydrogen bonds will make the backbone chains more coiled or even “crosslinked” with O=C(OH)—O=C(OH) groups; more —COOH groups are buried in the coiled chain aggregates, and not easy to enter the water phase. More H⁺ cations in the solution will protonate —COOH to produce —COOH₂⁺ groups on the backbone chains, as shown by Scheme 2. Electrostatic repulsion between these cations may prevent the —COOH groups from forming hydrogen bonds on both intramolecular and intermolecular chains, and make the backbone chains more extended, leading to a suspension of —COOH₂⁺ in an “isolated” state on the chains. In the studies of maleic anhydride copolymers, it has been known that if the ionization of —COOH groups is suppressed, the molecules acquire a random-coil conformation.²³ So, the hydrolyzed SMA in the acidified THF solution can show a much stronger emulsifying effect on the water phase than in a THF solution without HCl.

It is fact that a mixed solvent, consisting of THF and water, was used in preparing sample solutions for the HSMA film, even though the water quantity could be ignored. Compared with water, THF is of a much lower boiling point (i.e., 66°C/1 atm) and higher volatility, so the volatil-

ization process in spin-casting of HSMA solutions can be divided into two stages—THF and water volatilization. During the first stage, THF volatilized with water separating from the polymer, and the water phases were surrounded by the hydrolyzed SMA when the first stage finished; at the same time, the surfactant effect of hydrolyzed SMA leads to stable, well-arrayed, and uniform water droplets that contain chlorion (Cl^-) as counterions on their surface in the film. Then, water volatilized, and the whole volatilization stepped into the second stage. Finally, the holes were formed as traces of water phases when the second stage ended. As for the SMA- H_2O [Fig. 2(B)] and SMA [Fig. 2(A)] samples, it can be considered that there were no well-arrayed, droplet-like water domains in these two cases, for which the poor surfactant effect of SMA should be responsible.

The existence of water phases at hole sites can also be indicated by the influence of the water content on the hole size, as shown by Figure 6. The diameter and depth of holes increased with water content, but the number of holes reduced in the imaged area ($10 \times 10 \mu\text{m}^2$). As the weight ratio of the $\text{H}_2\text{O}/\text{SMA}$ increased from 1/3 to 1/1, the mean diameter of the holes increased from 1.11 to 1.23 μm , and the depth from 530 to 670 nm.

CONCLUSION

Distinct surface patterns in the thin films of poly(styrene maleic anhydride) spin-cast from different THF solutions were observed with AFM. Well-arrayed and almost uniform holes formed in the spin-cast thin films of hydrolyzed SMA. The formation of the holes was different from dewetting process in thin homopolymer films, but was associated with the intrinsic properties of the copolymer forming the films. The holes were interpreted as the traces of water droplets emulsified by the hydrolyzed SMA during casting. It still remains to be further investigated how the degree of hydrolysis of SMA influences the surface pattern of the thin film.

The authors appreciate the National Nature Science Foundation of China for supporting this work, and are grateful to Dr. Zheng Jiao (Hefei Institute of Intelligent Machine, Academia Sinica) for ellipsometric measurements of the films.

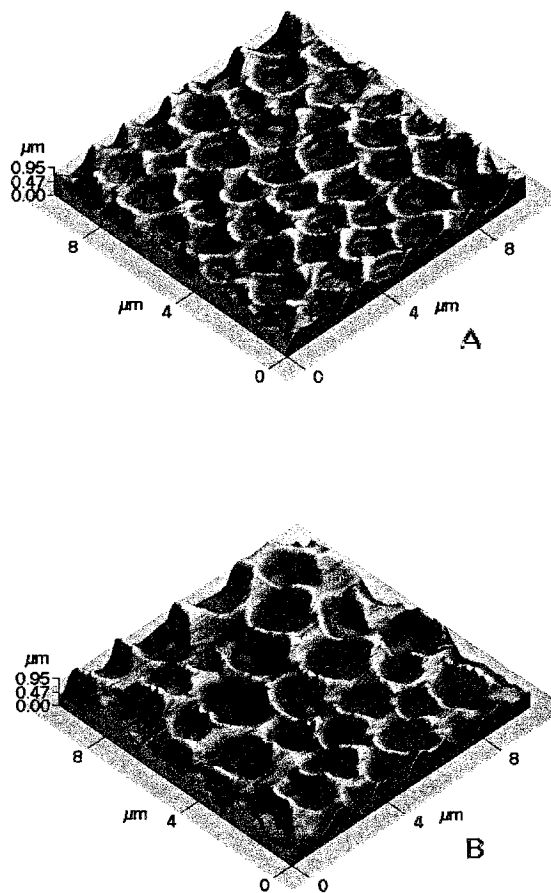


Figure 6 AFM images of thin films cast from HSMA solutions with a SMA concentration of 2% g/mL and different weight ratios of $\text{H}_2\text{O}/\text{SMA}$. (A) $\text{H}_2\text{O}/\text{SMA} = 1/3$; (B) $\text{H}_2\text{O}/\text{SMA} = 1/1$.

REFERENCES

1. Frank, C. W.; Rao, V.; Despotopoulou, M. M.; Pease, R. F. W.; et al. *Science* 1996, 273, 912.
2. Dalnoki-Veress, K.; Forrest, J. A.; Stevens, J. R.; Dutcher, J. R. *J Polym Sci Part B Polym Phys* 1996, 34, 3017.
3. Ermi, B. D.; Karim, A.; Douglas, J. F. *J Polym Sci Part B Polym Phys* 1998, 36, 191.
4. Karim, A.; Slawacki, T. M.; Kumar, S. K.; Douglas, J. F.; et al. *Macromolecules* 1998, 31, 857.
5. Tanaka, K.; Takahara, A.; Kajiyama, T. *Macromolecules* 1998, 31, 863.
6. (a) Kajiyama, T.; Tanaka, K.; Takahara, A. *Macromolecules* 1998, 31, 3746; (b) Li, Z.; Tolan, M.; Höhr, T.; Kharas, D.; et al. *Macromolecules* 1998, 31, 1916.
7. Affrossman, S.; Henn, G.; O'Neill, S. A.; Pethrick, R. A.; Stamm, M. *Macromolecules* 1996, 29, 5010.

8. (a) Reiter, G. *Langmuir* 1993, 9, 1344; (b) Reiter, G. *Phys Rev Lett* 1992, 68, 75.
9. Masuda, H.; Fukuda, K. *Science* 1995, 268, 1466.
10. Masuda, H.; Satoh, M. *Jpn J Appl Phys* 1996, 35, L126.
11. van Blaaderen, A.; Ruel, R.; Wiltzius, P. *Nature* 1997, 385, 321.
12. (a) Odian, G. In *Principles of Polymerization*; John Wiley & Sons: New York, 1981, 2nd ed.; (b) Tvivedi, B. C. In *Maleic Anhydride*; Plenum: New York, 1982.
13. (a) Ebdon, J. R.; Towns, C. R.; Dodgson, K. J. *Macromol Sci Rev* 1986, C26, 523; (b) Deb, P. C.; Meyerhoff, G. *Eur Polym J* 1984, 20, 713; (c) Tsuchida, E.; Tomono, T.; Sano, H. *Makromol Chem* 1972, 151, 245.
14. Barron, P. R.; Hill, D. J. T.; O'Donnell, J. H.; O'Sullivan, P. W. *Macromolecules* 1984, 17, 1967.
15. Braun, D.; Cherdron, H.; Kern, W. In *Techniques of Polymer Synthesis and Characterization*; John Wiley: New York, 1972.
16. Wang, M.; Zhu, X.; Wang, S.; Zhang, L. *Polymer* 1999, 40, 7387.
17. Hill, D. J. T.; O'Donnell, J. H.; O'Sullivan, P. W. *Macromolecules* 1985, 18, 9.
18. (a) Davis, F.; Hodge, P.; Towns, C. R.; et al. *Macromolecules* 1991, 24, 5695; (b) Prouchert, C. J. *The Aldrich Library of Infrared Spectra*, Aldrich Chemical Company, Inc. Milwaukee, WI, No. 20,061-1, 1981, III ed.
19. Shi, Y.; Sun, X.; Jiang, Y.; Zhao, T.; Zhu, H. In *The Spectroscopy and Chemical Identification of Organic Compounds*; Jiangsu Press of Science and Technology: Nanjing, 1988.
20. (a) Silverstein, R. M.; Bassler, G. C.; Morrill, T. C. In *Spectrometric Identification of Organic Compounds*; John Wiley & Sons, Inc.: New York, 1991; (b) Dyke, S. F.; Floyd, A. J.; Sainsbury, M.; Theobald, R. S. In *Organic Spectroscopy: An Introduction*; Longman Group Limited: London, 1978, 2nd ed.
21. Liu, C.; Jiang, X.; Li, B.; Zhang, W.; et al. In *Encyclopedia of Surfactant Application*; Press of Beijing University of Technology: Beijing, 1992, p. 47.
22. (Editorial Board: H. F. Mark, N. G. Gaylord, N. M. B. Kales). In *Encyclopedia of Polymer Science and Technology*; Interscience Publishers (a division of John Wiley & Sons, Inc.): New York, 1964, p. 81, vol. 1.
23. Reinhardt, S.; Steinert, V.; Werner, K. *Eur Polym J* 1996, 32, 939.